

Magnetic behaviour of the Cr-Al alloy system around the triple point

C J Sheppard¹, A R E Prinsloo, H L Alberts, A M Strydom and B Muchono
Department of Physics, University of Johannesburg, P O Box 524, Auckland Park,
Johannesburg, Republic of South Africa, 2006

E-mail: cjsheppard@uj.ac.za

Abstract. Electrical resistivity and specific heat measurements on a series of $\text{Cr}_{1-x}\text{Al}_x$ ($0 \leq x \leq 0.034$) alloy single crystals are reported. The results indicate that the triple point, where the incommensurate and commensurate spin-density-wave phases coexist with the paramagnetic phase, is situated close to $T = 0$ K on the magnetic phase diagram.

Introduction

The magnetic phase diagram of the itinerant electron alloy system $\text{Cr}_{1-x}\text{Al}_x$ presents a triple point at a concentration $x_c \approx 2$ at. % Al, where the incommensurate (I) and commensurate (C) spin-density-wave (SDW) antiferromagnetic (AF) phases coexist with the paramagnetic (P) phase [1]. Recent studies [2] on a $\text{Cr}_{0.978}\text{Al}_{0.022}$ alloy single crystal suggest that the triple point of the $\text{Cr}_{1-x}\text{Al}_x$ alloy series might be a special type of critical point, for which ISDW, CSDW and P phases coexist at 0 K. This suggestion is further investigated here through electrical resistivity (ρ) and specific heat (C_p) measurements on a series ($0 \leq x \leq 0.034$) of $\text{Cr}_{1-x}\text{Al}_x$ single crystals that include x_c .

Experimental techniques

The single crystals ($x = 0, 0.019, 0.022, 0.026, \text{ and } 0.034$) of this study were grown in our laboratories by a floating-zone technique using RF heating in an ultra-high purity argon atmosphere. Alloying Cr with Al forms dilute solid solutions in which Al atoms occupy substitutional sites in the body centred Cr lattice [3]. The as grown crystals were not submitted to applied magnetic fields and should be in the multi- \bar{Q} domain state, where \bar{Q} is the SDW wave vector. These crystals were previously used [4, 5, 6] for magnetoelastic (ME), neutron diffraction (ND) and in the case of $x = 0.022$ [2], also for $\rho(T)$ and $C_p(T)$ measurements. Measurements were done in the temperature range $2 \leq T \leq 350$ K, using standard PPMS [7] equipment. The electrical current for ρ measurements was directed along the cubic [100] crystallographic direction. The Sommerfeld specific heat coefficient (γ) was obtained for each x from a least squares fit to plots of C_p/T vs. T^2 at low temperatures. Such plots could be well fitted to the low-temperature approximation of the Debye formulation of specific heat $C_p(T) = \gamma T + \beta T^3$, where the first term represents the electronic specific heat component and the last term that of the acoustic modes of lattice contributions. Al impurities are not expected to produce local magnetic moments in Cr. Magnon contribution to C_p is therefore neglected in the above equation and γ is considered a measure of the density of states at the Fermi energy [8]. Theoretical models [9] for a simple two-lattice localized antiferromagnetic system predict a T^3 spin wave contribution to C_p , similarly to that of the

acoustic phonon contribution. In such an approximation an added magnon term to C_p will not influence γ .

Both ρ and γ are influenced by changes in the density of states at the Fermi energy. Such changes are introduced in Cr and its alloys by nesting of sections of the electron and hole Fermi surface sheets with a concomitant appearance of an energy band gap at the Fermi surface on SDW formation. These two physical parameters are thus ideally suited for the present investigation

Results

Figure 1 shows $\rho - T$ curves for the $\text{Cr}_{1-x}\text{Al}_x$ crystals. Although not too prominent for $x = 0.026$, these curves depict well defined $\rho(T)$ – anomalies of SDW origin below the Néel temperature (T_N), which is shown by an arrow at values previously [4, 5, 6] obtained from neutron diffraction and magnetoelastic measurements (or $\rho(T)$ - measurements in the case of pure Cr) on the same crystals. The crystals $x = 0$ and 0.019 display ISDW – P type Néel transitions [1, 5] and those with $x = 0.022, 0.26$ and 0.035 CSDW – P type [1, 4, 5], placing the $x = 0.022$ crystal probably just above the actual x_c .

The two ISDW alloys ($x = 0$ and 0.019) depict typical Cr-like $\rho(T)$ anomalies in the form of a hump, with or without a minimum point, on cooling through T_N . The three CSDW alloys, however, behave anomalously, depicting weaker anomalies at T_N , in contrast to observations on most other CSDW Cr alloys [1]. This is notwithstanding the presence of very strong magnetoelastic anomalies, pointing to the complexity of the magnetic behaviour of the Cr-Al system.

Figures 1 (a) and (b) also show base-line paramagnetic curves, $\rho_P(T)$, for the two $x = 0.019$ and 0.022 crystals, obtained from a theoretical back extrapolation of the $\rho(T)$ data at $T > T_N$ down to 0 K. The $\rho - T$ curves for figure 1 (b) and (c) were fitted rather well in the paramagnetic region $T > 100$ K using the equation [2]:

$$\rho_P(T) = \rho_0 + ATG\left(\frac{\theta_D}{T}\right) + BT^3, \quad (1)$$

where ρ_0 is the temperature independent impurity resistivity of an ideal non-magnetic $\text{Cr}_{1-x}\text{Al}_x$ crystal, the second term represents the lattice resistivity given by the Bloch-Grüneisen function $G(\theta_D/T)$, and the third term represents an electron s-d scattering term that plays a role in dilute Cr alloys [2]. ρ_0 , A , B , and θ_D were treated as fitting parameters for a best fit at $T > T_N$. These fitting parameters were then used to obtain $\rho_P(T)$ down to 2 K from equation (1). The back extrapolated $\rho_P(T)$ curves represent $\rho(T)$ should the two crystals remain paramagnetic down to 0 K in the absence of a P – SDW phase transition. Back extrapolation could however not be generated successfully for the other crystals, due the temperature range of the $\rho(T)$ measurements at $T > T_N$ being too small. For these the open symbol linear back extrapolations in figure 1 only serve as indications of the P-behaviour.

The results of figure 1 nevertheless indicate fairly good correspondence of T_N , obtained from neutron diffraction and magnetoelastic measurements, with the temperature where the magnetic contribution, $\Delta\rho(T) = \rho_{\text{measured}}(T) - \rho_P(T)$, tends to zero. This confirms a previous definition [2] of T_N for the $x = 0.022$ crystal and a much deeper and sharper minimum at the triple point on the SDW-P phase line of the magnetic phase diagram, than that generally accepted [1].

Good quality single crystalline Cr alloys, like Cr-Ru [10], usually present a small first-order like step in $\rho(T)$ on crossing the I-C phase line of the magnetic phase diagram. Such a step is absent in figure 1 for the CSDW alloys down to 2 K, confirming observations of neutron diffraction studies on the same crystals [4, 5] that the CSDW alloys remain CSDW without signs of an C-I transition down to 14 K. It is therefore concluded that, if present, the I-C phase line, starting at the triple point, (x_c, T_c), should have a very sharp slope, reaching a point ($x, 0$ K) in the range $0.019 < x < 0.022$, compared to the generally accepted [1] range $0.020 \lesssim x \lesssim 0.034$.

Figure 2(a) shows a plot of $\gamma(x)$ for the $\text{Cr}_{1-x}\text{Al}_x$ crystals, obtained from the $C_p(T)$ measurements at $T \leq 6$ K. Typical examples of low temperature linear $C_p(T)/T - T^2$ plots are shown in figures 2(a) and (b). Also shown in figure 2 are $\gamma(x)$ values [11] on polycrystalline $\text{Cr}_{1-x}\text{Al}_x$ alloys in the range $0 \leq x$

≤ 20 at.% Al. The present study gives decisive detail around x_c . Of importance is the sharp $\gamma(x)$ peak around $x \approx 0.025$, confirming a previous [2] conjecture in this regard.

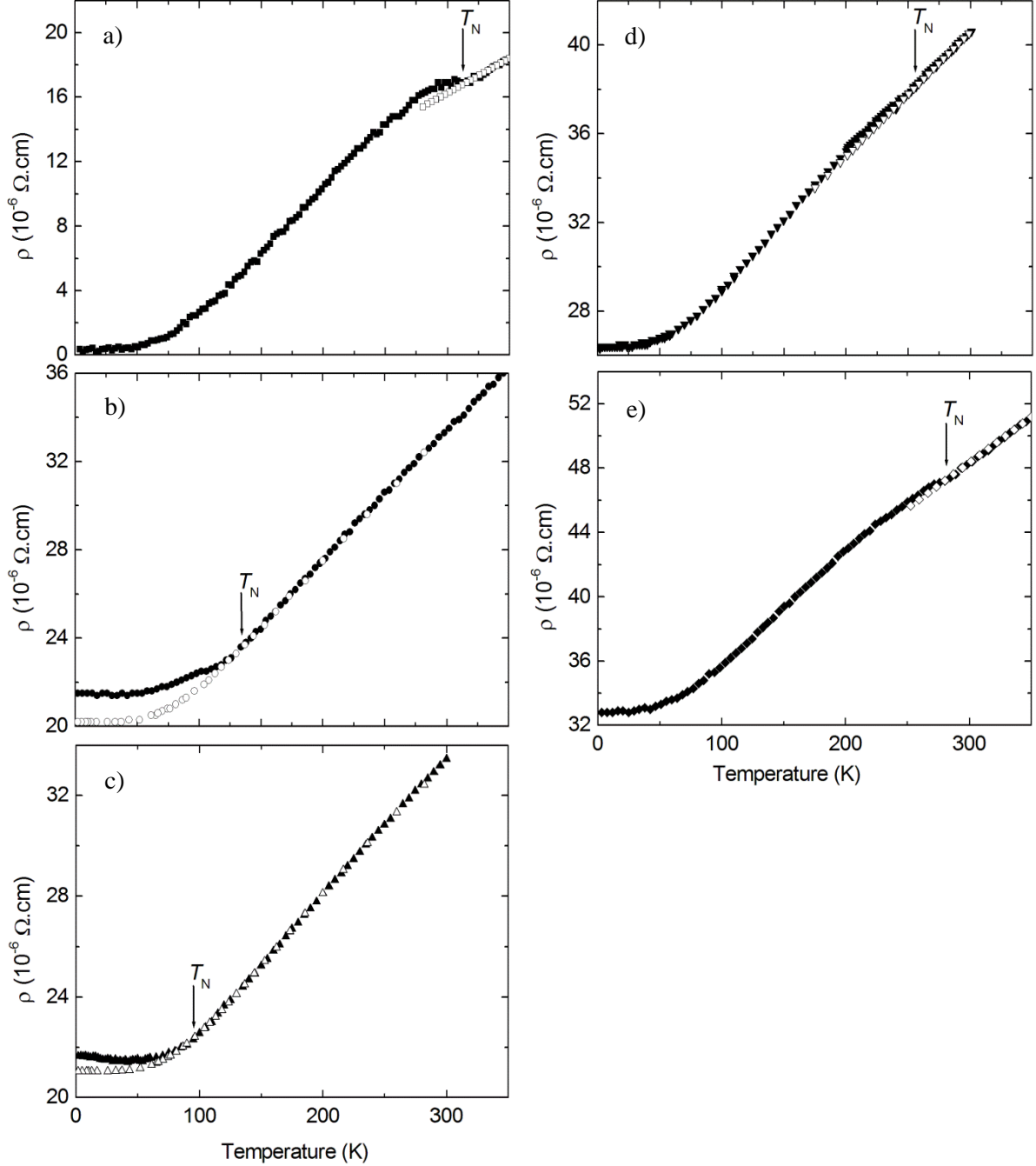


Figure 1: The electrical resistivity (ρ) as a function of temperature for $\text{Cr}_{1-x}\text{Al}_x$: (a) $x = 0$, (b) $x = 0.019$, (c) $x = 0.022$, (d) $x = 0.026$ and (e) $x = 0.034$. The arrows show the position of the Néel temperatures (T_N) obtained from magnetoelastic and neutron diffraction measurements. The open symbols for $x = 0.019$ and $x = 0.022$, depict the theoretical back extrapolated behaviour of each, should they remain paramagnetic down to 2 K [2]. The open symbols in (a), (d) and (e) only serve as “guides to the eye” back extrapolations, from the limited temperature range above the Néel transitions temperature.

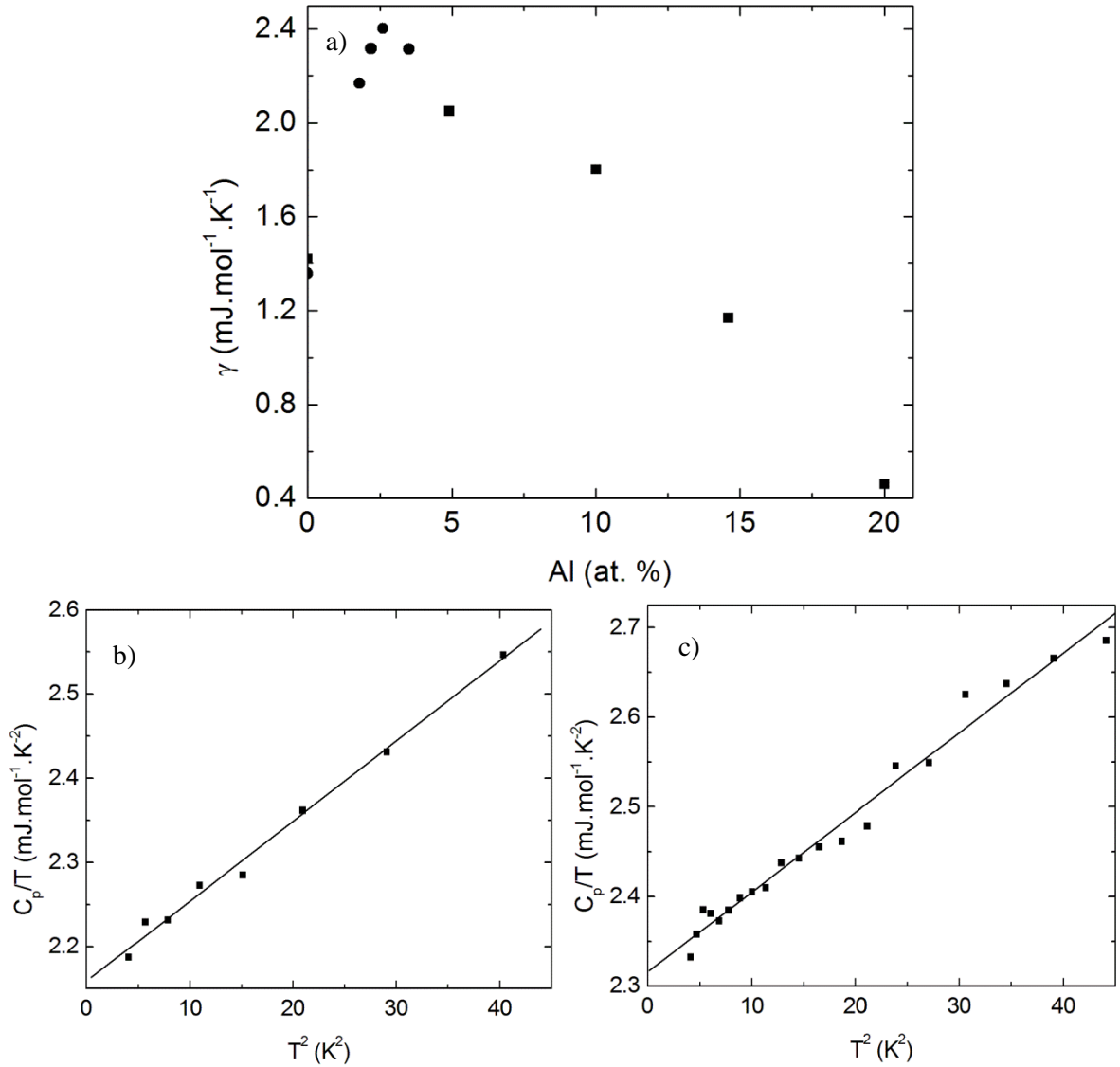


Figure 2: a) The Sommerfeld electronic specific heat coefficient (γ) as a function of Al-concentration for the $\text{Cr}_{1-x}\text{Al}_x$ alloy system: (●) present results, (■) Ref. [11]. Typical C_p/T vs. T^2 plot for b) $x = 0.019$ and c) $x = 0.034$ at low temperatures with the least-squares linear fit to the data points. The error within γ is within 0.2%.

It was previously [12] shown that the asymmetric $\gamma(y)$ peak observed in the $\text{Cr}_{1-y}\text{V}_y$ alloy system at the quantum critical point concentration, y_{QCP} , separating ISDW and P phases on the magnetic phase diagram at 0 K, is explained by combined influences of SDW energy gap and spin-fluctuation (SF) effects on $\gamma(y)$. In this system the slow decrease observed for $\gamma(y)$ in the P phase ($y \geq y_{\text{QCP}}$) is fully attributed to spin-fluctuation effects, while the sharp and large increase on increasing y up to y_{QCP} in the ISDW phase, mainly comes from effects of the SDW energy gap. We used this approach to interpret the sharp and large $\gamma(x)$ peak observed in figure 2.

In a scenario of a $\text{Cr}_{1-z}\text{Al}_z$ alloy system presenting a sequence ISDW-P-CSDW of phase transitions at 0 K on the magnetic phase diagram, one would, following the above discussion, expect $\gamma(z)$ to show two asymmetric peaks: one crossing the ISDW-P phase point and the other crossing the P-CSDW phase point on increasing z . $\gamma(z)$ should then increase sharply in the ISDW phase, followed

by a rather small variation in the P phase, and then by a down-turn as the CSDW phase is entered. Recent specific heat studies [13] in our laboratory show that this scenario is feasible in a $(\text{Cr}_{1-x}\text{Al}_x)_{95}\text{Mo}_5$ alloy system. If the width of the P phase region in this system could then be tuned to zero by tuning the Mo content, one would end up with a triple point at 0 K and a sharp peak in $\gamma(z)$, like that observed in the present $\text{Cr}_{1-x}\text{Al}_x$ system.

4. Conclusion

We presented a two-fold scenario for the behaviour of the $\text{Cr}_{1-x}\text{Al}_x$ alloy system around the triple point on the $T(x)$ magnetic phase diagram: either the phase boundary line separating ISDW and CSDW phases start at the triple point and reaches $T = 0$ K nearly vertically below this point, or this phase line is absent and the triple point is situated at or close to 0 K. The first scenario may be ruled out by the observation that a typical Cr alloy system with a triple point temperature $T > 300$ K and an I-C phase line that stretches towards 0 K over a relatively large concentration range, like the $\text{Cr}_{1-y}\text{Re}_y$ system, does not indicate a significant influence of the I-C transition on $\gamma(v)$ [14]. This is in contrast with the observation in figure 2(a) for $\text{Cr}_{1-x}\text{Al}_x$. The second scenario is, however, supported by the present $\gamma(x)$ and previous neutron diffraction measurements, making $\text{Cr}_{1-x}\text{Al}_x$ a likely candidate material exhibiting the enigmatic critical point where ISDW, CSDW and P phases coexist at 0 K.

5. Acknowledgements

Financial support from the SA National Research Foundation (Grant No's IFR2009021800008, 61388 and 2072956) is acknowledged. A. M. Strydom acknowledges financial support from UJ-URC.

6. References

- [1] Fawcett E, Alberts HL, Galkin V Yu, Noakes DR and Yakhmi JV 1994 Rev Mod. Phys. **66** 25
- [2] Alberts HL, Prinsloo ARE and Strydom AM 2010 J. Magn. Magn. Mater. **322** 1092
- [3] Takahashi J, Yamaguchi S, Fujino Y, Ozawa K, Mizuki J and Endoh Y 1980 J. Phys. Soc. Jpn. **49** 1480
- [4] Smit P, Alberts HL, Venter AM 2000 J. Appl. Phys. **87** 4885
- [5] Baran A, Alberts HL, Strydom AM, du Plessis P de V 1992 Phys. Rev. **B45** 10473
- [6] Alberts HL and Smit P 1995 Phys. Rev. **B51** 15146
- [7] Quantum Design, 6325 Lusk Boulevard CA 92121-3733, San Diego, USA]
- [8] Galkin V-Y, Ortiz WA, Black R, Diederichs J, Spanga S, Fawcett E 2003 Physica B **339** 137
- [9] Heiniger F, Bucher E, Muller J 1966 Phys. Kondens. Materie, **5**, 243
- [10] Smit P and Alberts HL 1993 J. Phys.: Condens. Matter **5** 6433
- [11] Pessal N, Gupta KP, Cheng CH and Beck P 1964 J. Phys. Chem. Solids **25** 993
- [12] Takeuchi J, Sasakura H and Masuda Y 1980 J. Phys. Soc. Jpn **49** 508
- [13] Muchono B 2011 private communication and presentation at this conference
- [14] Heiniger F 1966 Phys kondens. Materie **5** 286